J Mater Sci (2011) 46:2392–2396
DOI 10.1007/s10853-011-5258-5

LETTER

Properties of In-N doped ZnO films synthesized by ion beam assisted deposition

Zhi Yan · Xia Zhang · Yanhui Liu · Xiying Zhou · Jun Liang

Received: 8 September 2010 / Accepted: 6 January 2011 / Published online: 19 January 2011
© Springer Science+Business Media, LLC 2011

Introduction

ZnO has attracted more and more attention due to its wide band gap of 3.37 eV and large exciton of 60 meV [1, 2]. Now it is used widely in blue and ultraviolet light emitting devices [3]. For the development of ZnO-based optoelectronic devices, it is important to grow high quality of both p-type and n-type ZnO films. The n-type ZnO can easily be realized by Al [4, 5], In [6], or Sr [7] doping. However, it is rather difficult to fabricate p-type ZnO because ZnO is a natural n-type semiconductor due to the self-compensating effect. Theoretical calculations [8, 9] predict that nitrogen is the best dopant for p-type ZnO, because nitrogen may substitute oxygen in ZnO and act as acceptors. But the solution of nitrogen in ZnO is limited at very low level. Co-doping method of using acceptors and donors simultaneously has been introduced to increase the solution of N in ZnO [10, 11], whereas, N is still highly hard to doping.

Recently, several techniques have been used to prepare p-type ZnO, such as pulse laser deposition [12, 13], magnetron sputtering [14], ultrasonic spray pyrolysis [10], chemical vapor deposition [15], and molecular beam epitaxy [9], etc. In this study, the authors employed a new method of ion beam assisted deposition (IBAD) to prepare p-type ZnO through nitrogen ion beam of higher energy for doping. By this process, it can control precisely the final material properties such as microstructure, non-stoichiometry, and crystallinity. Hence the film will have high density, smooth morphology, and strong adherence between film and substrate [16]. Meanwhile, the ion beam bombardment on the growing film can enhance the arriving atoms mobility for crystallizing and even supply sufficient reactive atoms. So it may play important role in p-type doping ZnO film. Recently there are few researches on applying this method to realize p-type ZnO film [17]. In this study, p-type ZnO films with high carrier concentration are synthesized by ion beam assisted deposition and their post-annealing mechanism is studied.

Z. Yan (✉) · X. Zhang · Y. Liu · X. Zhou
Material Engineering College, Shanghai University of Engineering Science, Shanghai 201600, China
e-mail: yanzhik@126.com

J. Liang
State Key Laboratory of High Performance Ceramics and Superfine Microstructure, Shanghai Institute of Ceramics, Chinese Academy of Sciences, Shanghai 200050, China

Experiment

The deposition system used here was a dual-ion-beam system as shown in Fig. 1. The target for sputtering was a sintered ZnO (99.99% in purity) plates with 1 wt% In-doped. The substrates were silicon with 500 nm silicon dioxide and quartz crystal. Before deposition, the vacuum chamber was pumped to a base pressure of 6.0×10^{-4} Pa. The film preparation system consists of two Kaufman ion sources, one was used to sputter doped ZnO target with a 2 keV Ar^+ ion beam at average current density of 4.1 mA/cm^2 labeled gun I in Fig. 1. The other employed N_2 and O_2 mixing gas (1:1) to produce ion beam (N^+, O^+) of 5 keV with 4, 8, 1.6, and 0 μA/cm^2, respectively, to bombard the growing films labeled gun II. Ion bombardments at substrate can supply sufficient energies and reactive oxygen and doping nitrogen atoms to increase adatom mobility and chemical activity. During deposition, the temperature of substrate was about 100 °C and the work pressure was 6.1×10^{-3} Pa after pure NH_3 gas introduced into the chamber through the valve for N doping, as shown in Fig. 1.

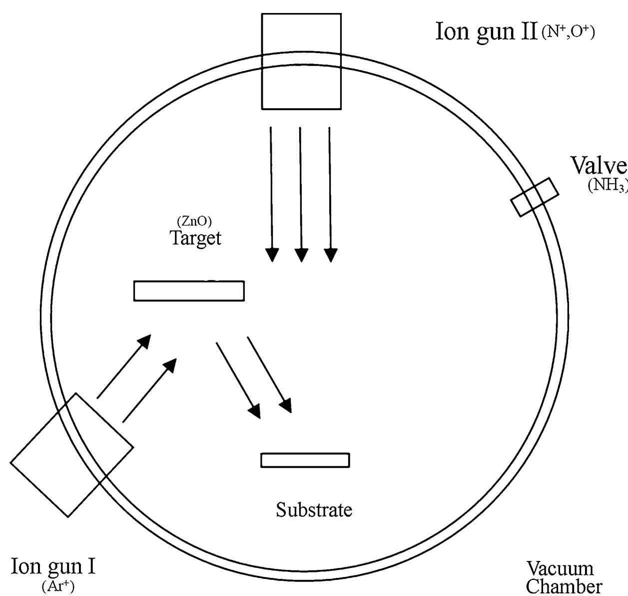

Fig. 1 A schematic diagram of the IBAD equipment used in this study

The deposition time was 6 h and the film thickness was about 500 nm. The synthesis conditions of the ZnO film were listed in Table 1. After deposition, the films were annealed by rapid thermal annealing in oxygen at temperature of 400 °C for 5, 15 and 30 min with a heating rate of 30°C/s. Hall effect measurements were carried out in the four probe van der Pauw method to test ZnO films at room temperature. The surface morphology of films was obtained by using field emission scanning electron microscopy (FE-SEM) and atomic force microscope (AFM). Their optical transmittance spectra were examined by spectrophotometer at room temperature.

Results and discussion

Data of Hall measurements for these films are listed in Table 2. The substrates used here are silicon with a layer of silicon oxidation in order to make sure that any p-type conduction coming from ZnO films rather than substrates Si. From Table 2, the carrier type of In-N doped ZnO film as deposited (sample A, E, and I) is n-type, with carrier concentration of 3.60×10^{17}, 7.30×10^{19}, and 3.74×10^{15} cm^{-3}, and with Hall mobility of 0.34, 19.65, and 18.3 cm^2/V s. It suggests that the ion bombardment energy plays an important role in film's electrical property. The carrier concentration in the film increases with ion gun energy, which demonstrates the advantage of ion assisted process for N and O ions doping. After annealing at 400 °C in O_2 for 5 and 15 min, these films (samples B, C and F, G) still remain n-type and Hall mobility increases along with the annealing time, while in contrary for carrier concentration. However, after annealing for 30 min, the conduction type of ZnO films shifts from n-type to p-type (sample D, H, and J). Thereby the p-type ZnO films can be synthesized by IBAD and post-annealing processing. In doping mechanism, the acceptor dopant N substitutes for O, and its chemical states in the ZnO films may be affected by indium incorporation and H combining. Moreover, the strong acceptor–donor attractive interaction overcomes the repulsive interactions between the acceptors to reduce the Madelung energies and to enhance the incorporation of acceptors, and then forms an acceptor–donor–acceptor complex in the band gap [18]. During the film deposition N acceptor, combining with H (from NH_3), is not electrical activated due to the low deposition temperature of substrates. This is hydrogen passivation. But ZnO native defects are active and more than that of N acceptors. Therefore, the n-type conduction of the films is observed. These films (samples B, C and F, G) are still kept in n-type probably because the N acceptors activation is insufficient, due to the annealing time is not long enough for atoms to diffuse to the right position and to break the N–H bonds. However, after a proper annealing time, the N–H bonds are broken and the N acceptors are activated. The ZnO native defects are either suppressed or not sufficient to compensate for N acceptors. So the conduction of these films (samples D, H, and J) is converted from n-type to p-type. The similar hydrogen passivation model has been interpreted in the literature [19]. Furthermore the carrier concentration decreases with the increase of annealing time in oxygen, because the chemisorbed oxygen trap density in samples deoxidized in this way is increased. The data obtained from the samples agree well with this argumentation.

SEM micrographs of these films are as shown in Fig. 2. Thickness of the film is about 500 nm from the

Table 1 Synthesis conditions of doped ZnO films by ion beam assisted deposition

Target	ZnO (doped In)	ZnO (doped In)	ZnO (doped In)	ZnO (doped In)
Substrate temperature (°C)	100	100	100	100
Base pressure (Pa)	6.0×10^{-4}	6.0×10^{-4}	6.0×10^{-4}	6.0×10^{-4}
Work pressure (Pa)	6.1×10^{-3} (filled NH_3)	6.1×10^{-3} (filled NH_3)	6.1×10^{-3} (filled NH_3)	6.1×10^{-3} (filled NH_3)
Sputtering ion beam (Gun I)	2 keV, 80 mA, Ar^+	2 keV, 80 mA, Ar^+	2 keV, 80 mA, Ar^+	2 keV, 80 mA, Ar^+
Bombarding ion beam (Gun II)	5 keV, 5 mA, N^+:O^+(1:1)	10 keV, 10 mA, N^+:O^+(1:1)	5 keV, 2 mA, N^+:O^+(1:1)	Without

Table 2 Electrical properties of doped ZnO films by ion beam assisted deposition

Sample	Gun II $N^+:O^+(1:1)$	Post-annealing	Resistivity (Ω cm)	Carrier concentration (cm^{-3})	Hall mobility ($cm^2\ V^{-1}\ s^{-1}$)	Type	RMS (nm)
A	5 keV, 5 Ma	Without	0.88	3.60×10^{17}	19.65	n	10.0
B	5 keV, 5 mA	400 °C, for 5 min	4.73	3.73×10^{16}	35.40	n	9.8
C	5 keV, 5 mA	400 °C, for 15 min	27.74	2.70×10^{16}	83.32	n	16.1
D	5 keV, 5 mA	400 °C, for 30 min	42.60	2.08×10^{15}	70.55	p	18.1
E	10 keV, 10 mA	Without	0.25	7.30×10^{19}	0.34	n	9.2
F	10 keV, 10 mA	400 °C, for 5 min	0.18	2.70×10^{19}	1.30	n	8.6
G	10 keV, 10 mA	400 °C, for 15 min	0.24	2.43×10^{19}	1.08	n	9.5
H	10 keV, 10 mA	400 °C, for 30 min	0.39	7.30×10^{18}	0.94	p	12.4
I	5 keV, 2 mA	Without	90.95	3.74×10^{15}	18.3	n	3.3
J	5 keV, 2 mA	400 °C, for 30 min	137.66	1.70×10^{15}	26.6	p	5.9
K	Without	Without	13.60	2.18×10^{17}	2.10	n	2.9
L	Without	400 °C, for 30 min	13.40	1.91×10^{17}	2.43	n	4.6

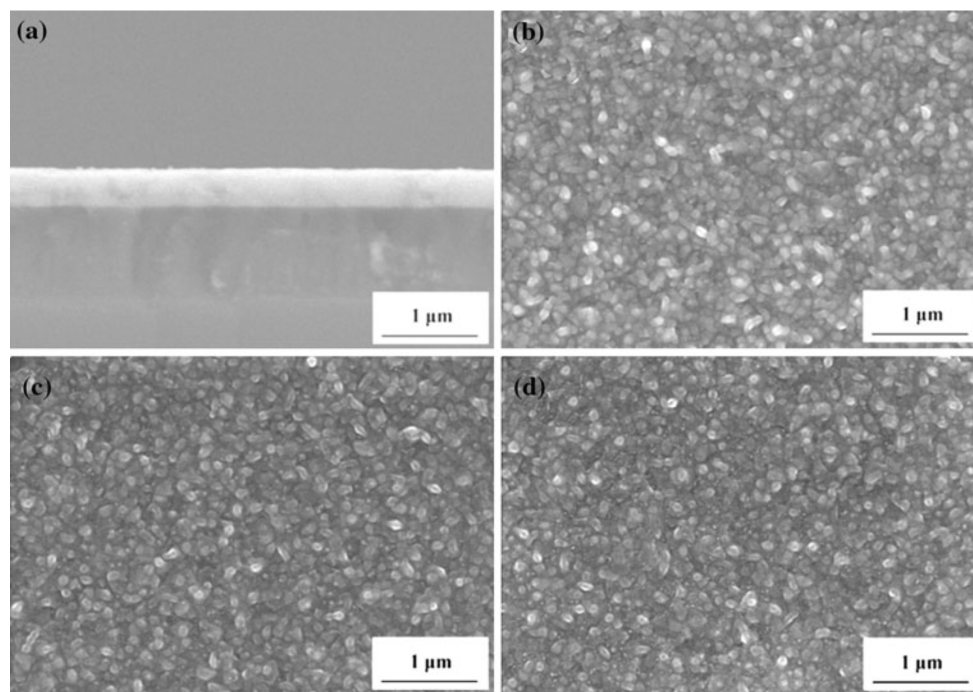

Fig. 2 SEM surface micrographs of In-N doping ZnO films with different post-annealing: **a** cross-section of the film (sample E), **b** as-deposited (sample E), **c** annealing at 400 °C for 15 min (sample G), and **d** annealing at 400 °C for 30 min (sample H)

cross-section micrograph. These films surface are composed of ZnO dense grains whose size averages from 100 to 200 nm. The SEM figures show that ZnO grain size changes little at different post-annealing time. Therefore, the size of ZnO grain still remains in its as-deposit size. Thus, the mobility increase tested in Hall effect is not justified by the increase in crystallite size and decrease in grain boundaries. The reason should be the decrease of impurity concentration as annealing time increase, thus increasing mobility.

Microstructure analysis of these films as deposited and after annealing is shown in Fig. 3 by AFM. From it, the morphology and the crystal grains do not change obviously after annealing. The roughness mean square (RMS) of the films (sample E to H) is 9.2, 8.6, 9.5, and 12.4 nm, respectively, increasing along with the annealing time, as well as samples A to D. The increase of surface roughness may cause more scattering of charge carriers, and increase the resistivity, as the data shown in Table 2.

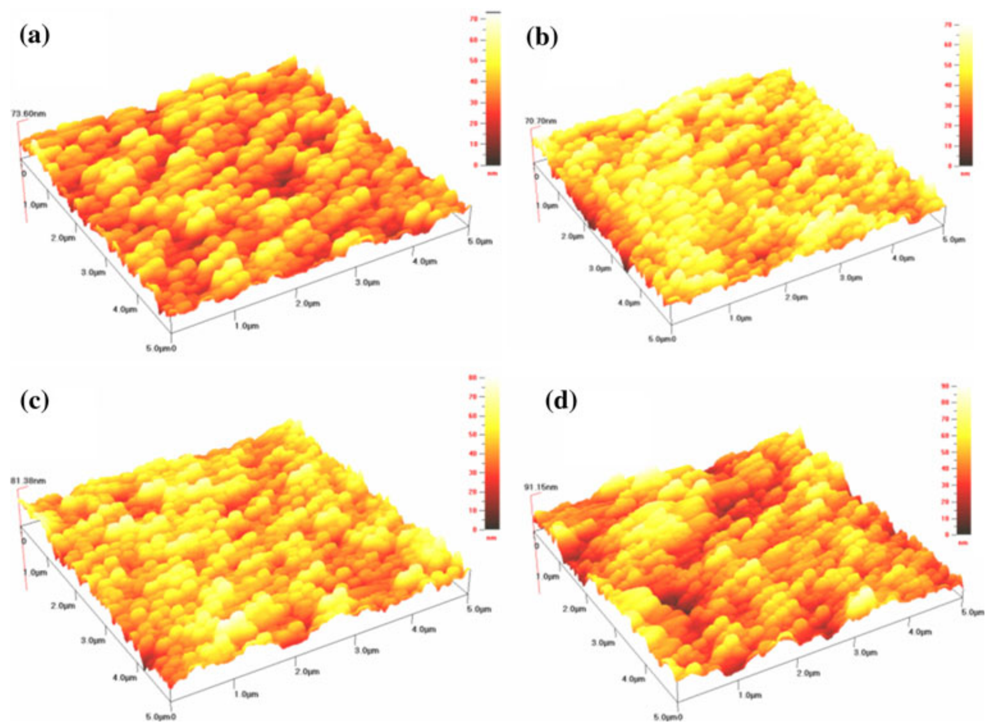

Fig. 3 AFM topographical maps of the In-N doping ZnO films with different post-annealing: **a** as-deposited (sample E), **b** annealing for 5 min (sample F), **c** annealing for 15 min (sample G), **d** annealing for 30 min (sample H). The surface root mean square roughness (RMS) values for these samples are 9.2 nm (**a**), 8.6 nm (**b**), 9.5 nm (**c**) and 12.4 nm (**d**)

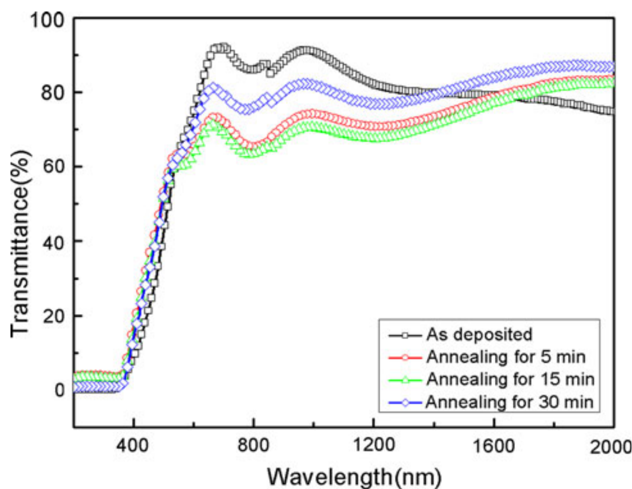

Fig. 4 Optical transmittance of In-N doped ZnO films grown on quartz crystal with different post-annealing

Figure 4 shows the transmission spectra of In-N co-doping ZnO films synthesized by IBAD on quartz crystal. The transmittance of as-deposited film (sample E) is about 85% in visible religion. With annealing in O_2, they (sample F, G) are decreased about 70%. But transmittance of the film (sample H) is increased about 80% again, with annealing for 30 min. Thus, post-annealing has an important effect on the transmittance for these films. As shown in Fig. 4, the absorption edges of these films are about 380 nm, near ultraviolet range, so that ZnO film has a very strong absorption property to ultraviolet light. The band gap energies of these films can be calculated using the absorption coefficient $\alpha \propto -\ln T(\lambda)$[20] and the absorption coefficient relation $\alpha h\nu = A(h\nu - E_g)^{1/2}$ [21], where $\nu = c/\lambda$. The optical band gap energies, E_g estimated are about 3.54, 3.48, 3.45, and 3.41 eV for sample E, F, G, and H, respectively. It suggests that the optical band gap is decreased with increasing annealing time. The variation in band gap energy (the ZnO, $E_g$of 3.37 eV) may be related with the degree of non-stoichiometry in ZnO and doping dopant incorporation [22]. After annealing the ZnO film has less degree of non-stoichiometry and more degree of doping dopant incorporation, so the band gap energy changes.

Conclusions

In summary, the authors have fabricated p-type ZnO films by adopting ion beam assisted deposition and post-annealing. These films demonstrate n-type at first. With post-annealing in O_2 at 400 °C for 30 min, the conduction of the films converts to p-type. The post-annealing plays an important role on the film electrical and optical properties. The optical properties show blue shift along with annealing time. Meanwhile, the surfaces of these films show high stable qualities and no obvious morphology change happens after annealing.

Acknowledgements This study is supported by Innovation Program (08YZ157), (07-24) of Shanghai Municipal Education Commission and Shanghai Leading Academic Discipline Project (J51402).

References

1. Look DC, Reynolds DC, Sizelove JR, Jones RL, Litton CW, Cantwell G, Harsch WC (1998) Solid State Commun 105:399
2. Tang ZK, Wong GKL, Yu P, Kawasaki M, Ohtomo A, Koinuma H, Segawa Y (1998) Appl Phys Lett 72:3270
3. Patil SB, Singh AK (2010) J Mater Sci 45:5204. doi:10.1007/s10853-010-4559-4
4. Kim H, Gilmore CM, Horwitz JS (2000) Appl Phys Lett 76:259
5. Park KC, Ma Y, Kim KH (1997) Thin Solid Films 305:201
6. Nunes P, Fortunato E, Martins R (2000) Thin Solid Films 383:277
7. Vijayan TA, Chandramohan R, Valanarasu S, Thirumalai J, Subramanian SP (2008) J Mater Sci 43:1776. doi:10.1007/s10853-007-2404-1
8. Park CH (2002) Phys Rev B 66:073202
9. Li L, Shan CX, Li BH, Zhang JY, Yao B, Shen DZ, Fan XW, Lu YM (2010) J Mater Sci 45:4093. doi:10.1007/s10853-010-4497-1
10. Wang B, Zhao Y, Min J, Sang W (2009) Appl Phys A 94:715
11. Shet S, Ahn KS, Wang H, Nuggehalli R, Yan Y, Turner J, Jassim MA (2010) J Mater Sci 45:5218. doi:10.1007/s10853-010-4561-x
12. Kim H, Cepler A, Cetina C, Knies D, Osofsky M, Auyeung R, Piqué A (2008) Appl Phys A 93:593
13. Tien LC, Pearton SJ, Norton DP, Ren F (2008) J Mater Sci 43:6925. doi:10.1007/s10853-008-2988-0
14. Lu JG, Zhu LP, Ye ZZ, Zhuge F, Zeng YJ, Zhao BH, Ma DW (2005) Appl Surf Sci 245:109
15. Minegishi K, Koiwai Y, Kikuchi Y, Yano K, Kasuga M, Shimizu A (1997) Jpn J Appl Phys 36:1453
16. Yan Z, Song ZT, Liu WL, Wan Q, Zhang FM, Feng SL (2005) Thin Solid Films 492:203
17. Yuan NY, Fan LN, Li JH, Wang XQ (2007) Appl Surf Sci 253:4990
18. Yamamoto T, Yoshida HK (2001) Phys B 302:155
19. Ogata KI, Kawaguchi D, Kera T, Fujita S, Fujita S (1996) J Crystal Growth 159:312
20. Shan FK, Kim BI, Liu GX, Liu ZF, Sohn JY, Lee WJ, Shin BC, Yu YS (2004) J Appl Phys 95:4772
21. Chaabouni F, Abaab M, Rezig B (2004) Mat Sci Eng B 109:236
22. Aly SA, Sayed NZE, Kaid MA (2001) Vacuum 61:1